5th International Conference on Mathematical Modeling in Physical Sciences (IC-MSquare 2016) IOP Publishing
Journal of Physics: Conference Series **738** (2016) 012112 doi:10.1088/1742-6596/738/1/012112

Numerical simulation of steady and unsteady flow for generalized Newtonian fluids

Radka Keslerová, David Trdlička, Hynek Řezníček

Czech Technical University in Prague, Faculty of Mechanical Engineering, Dep. of Technical Mathematics, Czech Republic

E-mail: Radka.Keslerova@fs.cvut.cz, David.Trdlicka@fs.cvut.cz, Hynek.Reznicek@fs.cvut.cz

Abstract. This work presents the numerical solution of laminar incompressible viscous flow in a three dimensional branching channel with circle cross section for generalized Newtonian fluids. The governing system of equations is based on the system of balance laws for mass and momentum. Numerical solution is based on cetral finite volume method using explicit Runge-Kutta time integration. In the case of unsteady computation artificial compressibility method is considered.

1. Introduction

Branching of pipes occurs in many technical or biological applications. In [14] the effects of viscoelasticity on the pitchfork bifurcation using a numerical finite volume method was investigated. Results from both the upper-convected Maxwell and Oldroyd-B models show that the instability occurs at lower Reynolds numbers for viscoelastic fluids in comparison to the Newtonian base case. In [13] computational fluid dynamics simulations of steady viscoelastic flows through a planar two dimensional T-junction is considered and the influence of constitutive model and fluid elasticity upon the main recirculating flow characteristics formed at the junction and the shear stress fields is studied. In biomedical applications, it is the complex branching system of blood vessels in human body. The blood can be characterized by shear-thinning viscoelastic property and the blood flow can be described by generalized Oldroyd-B model. In [1] the new model to describe the rheological characteristics of blood (namely shear-thinning and deformation dependent viscoelasticity) in both steady and unsteady flows was developed. In [3] a comparative numerical study of non-Newtonian fluid models capturing shear-thinning and viscoelastic effects of blood flow in idealized and realistic stenosed vessels was presented. In [16] a novel, time-accurate approach for solving the unsteady incompressible NavierStokes equations on non-staggered grids is proposed. The approach modifies the standard, dual-time stepping artificial-compressibility iteration scheme by incorporating ideas from pressure-based, fractional-step formulations.

In prewious work we studied the numerical simulation of generalized Newtonian and Oldroyd-B fluids flow in 2D branching channel, [8], [9]. In this article the problem of the unsteady numerical simulation for the generalized Newtonian fluids flow is presented. The modelled domain is the three dimensional branching channel with T-junction.


Content from this work may be used under the terms of the Creative Commons Attribution 3.0 licence. Any further distribution of this work must maintain attribution to the author(s) and the title of the work, journal citation and DOI.
Published under licence by IOP Publishing Ltd

2. Mathematical model

The governing system of equations is the system of generalized Navier-Stokes equations, see [2], [12]. This system consists of the continuity equation and the momentum equation

$$\text{div } \boldsymbol{u} = 0 \tag{1}$$

$$\rho\frac{\partial \boldsymbol{u}}{\partial t} + \rho(\boldsymbol{u}.\nabla)\boldsymbol{u} = -\nabla P + \text{div } \mathbf{T}, \tag{2}$$

where P is the pressure, ρ is the constant density, $\boldsymbol{u}$ is the velocity vector. The symbol $\mathbf{T}$ represents the stress tensor.

The stress tensor $\mathbf{T}$ is defined by corresponding rheological model, Newtonian, see e.g. [1], [3], [4], [5], [8]

$$\mathbf{T} = 2\mu_s\mathbf{D} \tag{3}$$

where μ_s is the dynamic fluid viscosity and tensor $\mathbf{D}$ is the symmetric part of the velocity gradient, $\mathbf{D} = \frac{1}{2}(\nabla\boldsymbol{u} + \nabla\boldsymbol{u}^T)$.

For the numerical modelling of the generalized Newtonian fluids flow it is necessary to generalize the mathematical model. The constant viscosity coefficient μ_s is replaced by a shear rate dependent viscosity function $\mu(\dot\gamma)$ where shear rate $\dot\gamma$ is defined by $\dot\gamma = 2\sqrt{\frac{1}{2}\text{tr } \mathbf{D}^2}$. This function can be written in the following general form (for more details see [15], [17])

$$\mu(\dot\gamma) = \mu_\infty + \frac{\mu_0 - \mu_\infty}{(1 + (\lambda\dot\gamma)^b)^a}, \quad \dot\gamma = 2\sqrt{\frac{1}{2}\text{tr } \mathbf{D}^2}, \tag{4}$$

with special parameters $\mu_0 = 1.6 \cdot 10^{-1} Pa.s, \mu_\infty = 3.6 \cdot 10^{-3} Pa.s, a = 1.23, b = 0.64, \lambda = 8.2s$. For Newtonian flow, the viscosity μ_s is kept constant and equal to μ_∞.

3. Numerical solution

The mathematical models described above are solved numericaly the artificial compressibility approach combined with the finite-volume discretization. The artificial compressibility method [6], [8], [12] is used to obtain equation for pressure. It means that the continuity equation is completed by a pressure time derivative term $\frac{\partial p}{\beta^2\partial t}$, where β is positive parameter, making the inviscid part of the system of equations hyperbolic. The parameter β for steady case is chosen equal to the maximum inlet velocity. This value ensures good convergence to steady state but is not large enough to make the transient solution accurate in time. Therefore it is suitable for steady flows only. In the case of unsteady simulation this parameter is 100x higher. The discretization is done by a cell-centered finite-volume method with hexahedral finite volumes. The system including the modified continuity equation and the momentum equations can be written

$$\tilde R_\beta W_t + F_x^c + G_y^c + H_z^c = F_x^v + G_y^v + H_z^v, \quad \tilde R_\beta = \text{diag}(\frac{1}{\beta^2}, 1, \cdots, 1), \tag{5}$$

where W is vector of unknowns, $W = (p, u, v, w)$, by superscripts c and v the inviscid and the viscous fluxes are denoted. Eq. (5) is discretized in space by the finite volume method and the arising system of ODEs is integrated in time by the explicit multistage Runge–Kutta scheme ([8], [11]).

The flow is modelled in a bounded computational domain where a boundary is divided into three mutually disjoint parts: a solid wall, an outlet and an inlet. At the inlet Dirichlet boundary condition for velocity vector is used and for the pressure homogeneous Neumann boundary condition is used. At the outlet parts the pressure value is prescribed and for the velocity vector homogeneous Neumann boundary condition is used. The no-slip boundary condition for the velocity vector is used on the wall. For the pressure homogeneous Neumann boundary condition is considered.

3.1. Unsteady computation

For numerical solution of unsteady flows the artificial compressibility method is applied. In this case the artificial compressibility parameter β is set to be 100x higher than for steady case. The question arises, how big the parameter β should be in numerical calculations. Numerical calculations show, that $\beta = 6\text{m s}^{-1}$ is the proper choice. The artificial compressibility approach used for unsteady incompressible flows is modifying the system of equations by adding an unsteady term to the continuity equation in the same way as for steady case, see e.g. [7].

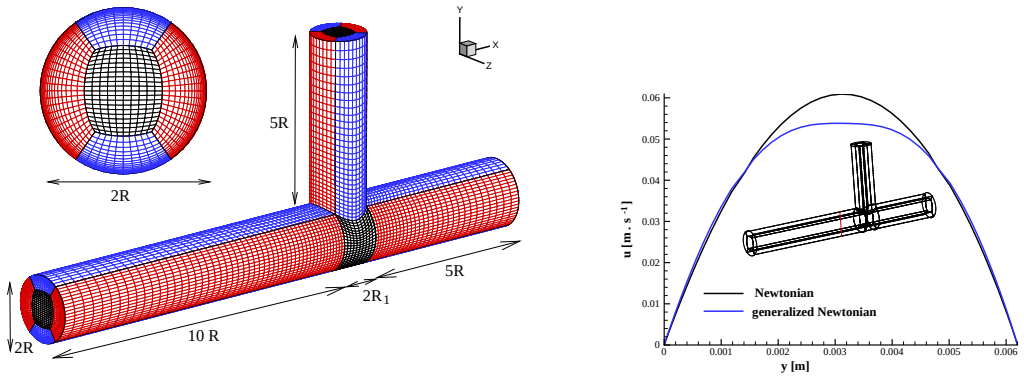
The unsteady boundary conditions are defined as follows. In the inlet, in the solid wall and in one of the outlet part the steady boundary conditions are prescribed. In the second outlet part (the branch) new boundary condition is defined. The pressure value is prescribed by the function

$$p_{branch} = \frac{1}{4}\left(1 + \frac{1}{2}\sin(\omega t)\right), \tag{6}$$

where ω is the angular velocity defined as $\omega = 2\pi f$, where f is a frequency. In this work these values of the frequency are tested: $f = 2, 5, 10, 20, 50, 100$ Hz.

4. Numerical Results

This section deals with the comparison of the numerical results of Newtonian and generalized Newtonian fluids flow. Numerical tests are performed in an idealized branched channel with the circle cross-section. Fig. 1 (left) shows the shape of the tested domain. The computational domain is discretized using a structured, wall fitted mesh with hexahedral cells. The domain is divided to 19 blocks with 125 000 cells.



(a) structure of the domain (b) axial velocity profile

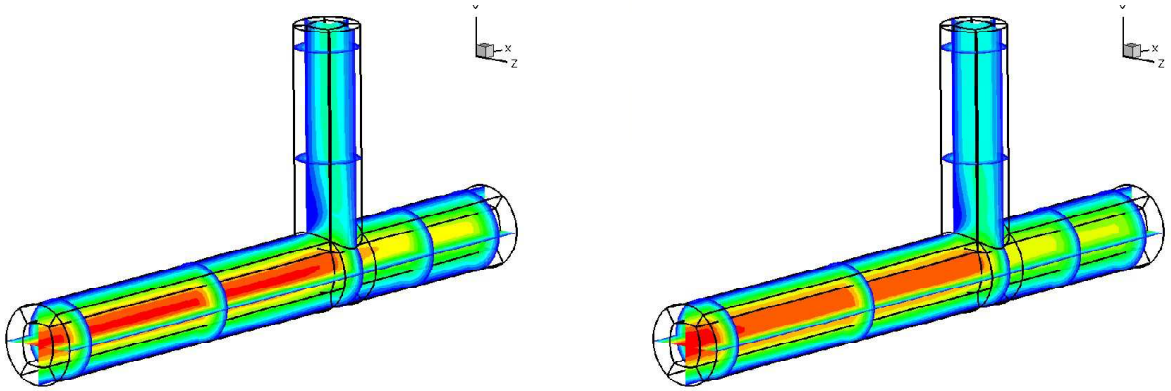
Figure 1. Structure of the tested domain (left) and axial velocity profile of tested fluids (right).

All numerical results presented in this section were computed using in-house software. The computational code was verified for the steady flow of an incompressible fluid in a straight tube by prescribing a constant velocity profile at the inlet. Fully developed velocity profiles for all tested fluids were used as the initial velocity profile for following computations in the branching channel with T-junction. At the outlet the constant pressure values are prescribed (0.0005 Pa (main channel) and 0.0005 Pa (branch)).

The computations were performed with the following model parameters: $R = 0.0031$ m, $R_1 = 0.0025$ m, $\mu_s = 0.0036$ Pa s, $U_0 = 0.0615$ m s^{-1}, $\rho = 1050$ kg m^{-3}. In Fig. 1 the axial velocity profile for tested types of fluids close to the branching is shown. The lines for Newtonian fluids are similar to the parabolic line, as was assumed. From this velocity profile is clear that the shear thinning fluids attain lower maximum velocity in the central part of the channel (close

to the axis of symmetry) which is compensated by the increase of local velocity in the boundary layer close to the wall.

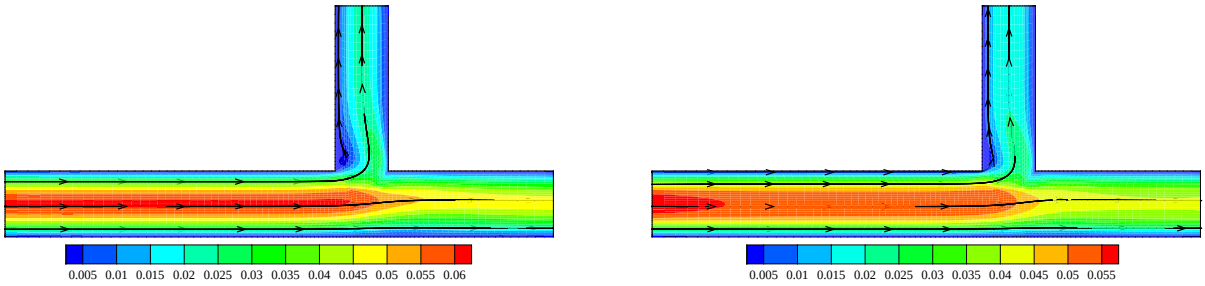
In Figs. 2 the velocity isolines and the cuts through the main channel and the small branch are shown.



(a) Newtonian (b) generalized Newtonian

Figure 2. Velocity isolines of steady flows for generalized Newtonian fluids.

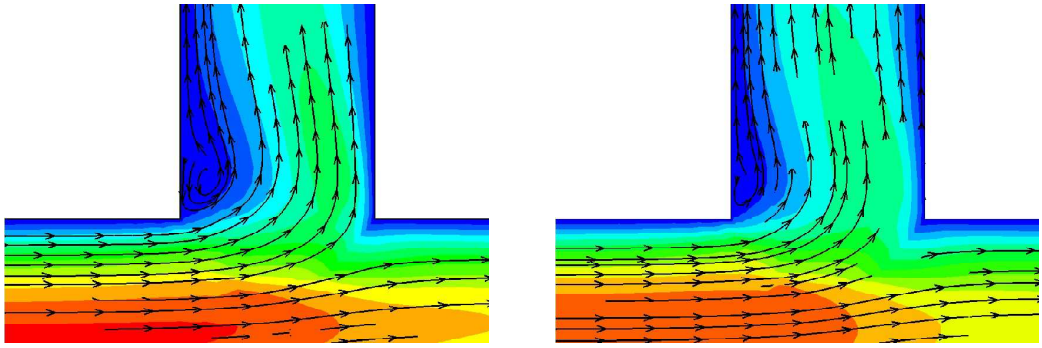
The axial velocity isolines in the center-plane area for all tested fluids are shown in the Figs. 3. It can be observed from these that the size of separation region for generalized Newtonian fluids is smaller than for Newtonian fluids, see in detail Fig. 4.



(a) Newtonian (b) generalized Newtonian

Figure 3. Axial velocity isolines in the center-plane area for generalized Newtonian fluids.

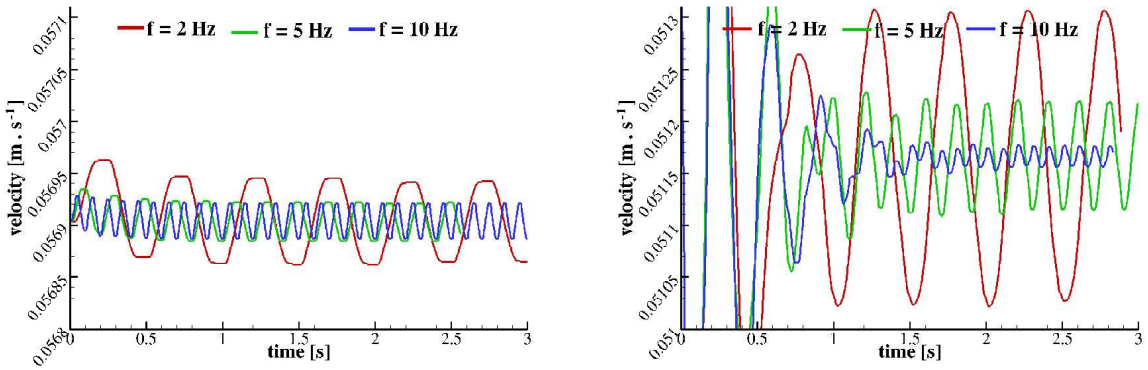
These steady numerical results are used as initial condition for unsteady numerical computation. The artificial compressibility method is used for the unsteady numerical simulation of generalized Newtonian fluids flow in the branching channel with T-junction with circle cross section. In this case the unsteady boundary condition are considered. It means that the pressure value in the branch outlet part is changing with given pressure function 6. Six values of frequency are tested, $f = 2, 5, 10, 20, 50, 100$ Hz. Parameter β is set to be 100x higher than for steady case, $\beta = 6.0$ m s^{-1}.



(a) Newtonian (b) generalized Newtonian

Figure 4. Axial velocity isolines in the center-plane area in the separation region.

In Fig. 5 and 6 graphs of velocity as the function of time for lower and higher values of the frequency are shown.



(a) Newtonian (b) generalized Newtonian

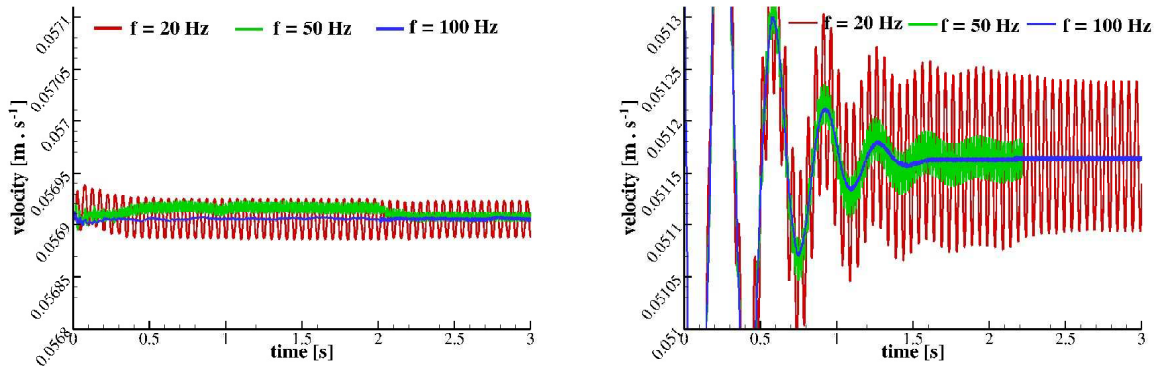
Figure 5. The graphs of the velocity as the function of time for lower values of frequency.

5. Conclusion

Classical Newtonian, as well as its generalized (shear-thinning) modification have been considered to model flow in the branching channel with T-junction, to investigate shear-thinning effects in steady flow simulations. From the presented velocity profile is clear that the shear thinning fluids (generalized Newtonian fluids) attain lower maximum velocity in the central part of the channel (close to the axis of symmetry) which is compensated by the increase of local velocity in the boundary layer close to the wall.

The numerical method used to solve the governing equations seems to be sufficiently robust and efficient for the appropriate resolution of the given class of problems.

One approach was considered for numerical solution of unsteady governing equations - an artificial compressibility approach. The artificial compressibility parameter β set to be $6ms^{-1}$. Several values for frequency were tested. Pressure value in the branch outlet was prescribed by periodic function. The numerical results given by graphs of the velocity as the function of the time were presented.



(a) Newtonian (b) generalized Newtonian

Figure 6. The graphs of the velocity as the function of time for higher values of frequency.

For the future work the extending this unsteady simulation for generalized Oldroyd-B fluids flow is considered. The new unsteady method, dual-time stepping method, will be used.

Acknowledgments
This work was supported by the grant SGS16/206/OHK2/3T/12.

References
[1] Anand M, Kwack J and Masud A 2013 *International Journal of Engineering Science* **72** 78–88
[2] Beneš L, Louda P, Kozel K, Keslerová R and Štigler J 2013 *Applied Mathematics and Computation* **219** 7225–7235
[3] Bodnar T, Sequeira A and Prosi M 2010 *Applied Mathematics and Computation* **217** 5055–5067
[4] Bodnar T and Sequeira A 2010 *Advances in Mathematical Fluid Mechanics* 83–104
[5] Bodnar T, Sequeira A and Pirkl L 2009 *In Numerical Analysis and Applied Mathematics* **2** 645–648
[6] Chorin AJ 1967 *Journal of Computational Physics* **135** 118–125
[7] Gaitonde AL 1998 *Intern. Journal for Numerical Methods in Engineering* **41** 1153–1166
[8] Keslerová R and Kozel K 2012 *Proc. 16th Sem. on Programs and Algorithms of Num. Math.* (Inst. of Math. Ac. of Sc. of CR) 100
[9] Keslerová R and Kozel K 2011 *Proc. 6th Intern. Symposium on Finite Volumes for Complex Applications* (Berlin: Springer) 589
[10] Leuprecht A and Perktold K 2001 *Computer Methods in Biomechanics and Biomechanical Engineering* **4** 149–163
[11] LeVeque R 2004 *Finite-Volume Methods for Hyperbolic Problems* (Cambridge University Press)
[12] Louda P, Kozel K, Příhoda J and Sváček P 2013 *International Journal of Heat and Fluid Flow* **43** 268–276
[13] Matos HM and Oliveira PJ 2014 *Journal of Non-Newtonian Fluid Mechanics* **213** 15–26
[14] Poole RJ, Haward SJ and Alves MA 2014 *Procedia Engineering* **79** 28–34
[15] Rabby MG, Razzak A and Molla MM 2013 *Procedia Engineering* **56** 225–231
[16] Tang HS and Sotiropoulos F 2007 *Computers and Fluids* **36** 974–986
[17] Vimmr J, Jonášová A and Bublík O 2010 *Mathematics and Computers in Simulation* **80** 1324–1336